JOC*Article*

A DFT Study on the Mechanism of Hydrosilylation of Unsaturated Compounds with Neutral Hydrido(hydrosilylene)tungsten Complex

Xin-Hao Zhang,[†] Lung Wa Chung,[†] Zhenyang Lin,*[,†] and Yun-Dong Wu*[,†,‡]

Department of Chemistry, The Hong Kong University of Science and Technology, Clear Water Bay, Kowloon, Hong Kong, China, and State Key Laboratory of Molecular Dynamics and Stable Structures, College of Chemistry, Peking University, Beijing, China

chydwu@ust.hk; chzlin@ust.hk

Received July 27, 2007

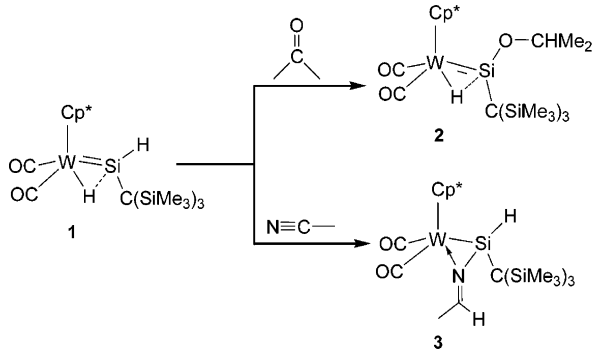

Recently, Tobita et al. reported stoichiometric hydrosilylation reactions of acetone and acetonitrile with neutral hydrido(hydrosilylene)tungsten complexes $Cp'(CO)_2(H)W{=}Si(H)[C(SiMe_3)_3]$ ($Cp' = Cp^*$, C_5Me_4Et). The mechanisms of the hydrosilylation reactions of unsaturated compounds (ketone and nitrile) with the tungsten complexes have been investigated with the B3LYP density functional theory method. Four possible reaction mechanisms were studied. The results of the calculations indicate that the hydrosilylation of acetone proceeds via a metal hydride migration mechanism proposed by Tobita et al., while the hydrosilylation of nitrile occurs through a silyl migration mechanism, analogous to the modified Chalk−Harrod mechanism. The $[2_\sigma+2_\pi]$ additions of various CX (CX = C=O or C≡N) multiple bonds with the Si−H bonds in the neutral complexes have very high barriers although similar additions were found feasible in other related cationic complexes. All the hydrosilylation reactions studied here give stable tungsten−silylene or tungsten−silyl products, which are not easily converted into the starting hydrido(hydrosilylene)tungsten complexes when reacting with a hydrosilane substrate molecule. Therefore, we predict that hydrosilylation of acetonitrile and acetone catalyzed by these tungsten complexes is difficult to achieve.

Introduction

Hydrosilylation reactions of alkenes, alkynes, and carbonyl compounds have been extensively studied because these reactions provide straightforward and atom-economical methods for the generation of versatile organosilicon compounds.[1] Transition metal silylene complexes, as silicon analogues of metal carbenes, are proposed as important intermediates in many metal-catalyzed transformations of organosilicon compounds.[2] Recently, Glaser and Tilley developed cationic ruthenium−silylene complexes which are capable of catalyzing regioselective anti-Markovnikov hydrosilylation of alkenes. They proposed a mechanism involving a $[2_\sigma+2_\pi]$ addition between the Si−H bond of the silylene ligand in the cationic complex and the alkene C=C double

* To whom correspondence should be addressed.
[†] The Hong Kong University of Science and Technology.
[‡] Peking University.

(1) (a) Ojima, I. In *The Chemistry of Organosilicon Compounds*; Patai, S., Rappoport, Z., Eds.; John Wiley & Sons: Chichester, UK, 1989; pp 1479−1526. (b) Ojima, I.; Li, Z.; Zhu, J. In *The Chemistry of Organosilicon Compounds*; Rappoport, Z., Apeloig, Y., Eds.; John Wiley & Sons: Chichester, UK, 1998; Vol. 2, pp 1687−1792. (c) Hiyama, T.; Kusumoto, T. In *Comprehensive Organic Synthesis*; Trost, B. M., Fleming, I., Eds.; Pergmon Press: Oxford, UK, 1991; Vol. 8, pp 763−792. (d) Ball, Z. T. In *Comprehensive Organometallic Chemistry III*; Crabtree, R. H., Mingos, M., Eds.; Elsevier: Oxford, UK, 2007; Vol. 10, p 789.

10.1021/jo701649m CCC: $40.75
Published on Web 12/28/2007

SCHEME 1. The Mechanism for the Stoichiometric Hydrosilylation Reactions (Eqs 1 and 2) Proposed by the Tobita Group

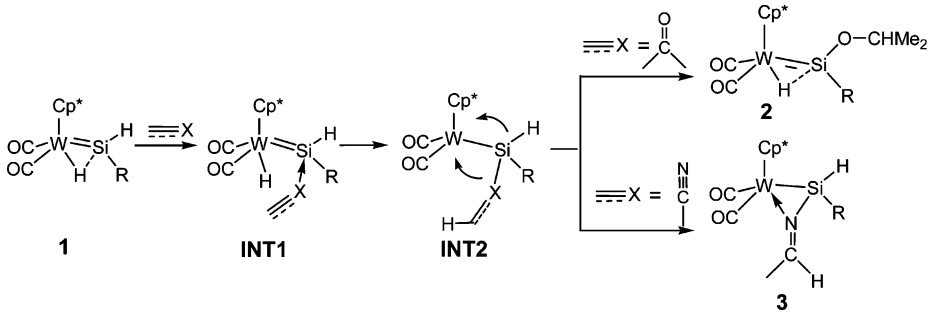

bond.[3] This mechanism was later supported by theoretical investigations.[4,5] This discovery demonstrated the potential role of transition metal−silylene complexes in catalytic hydrosilylations.

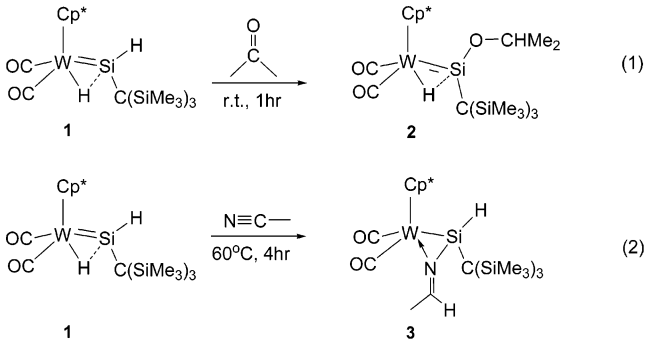

More recently, Tobita and co-workers reported the synthesis and characterization of neutral base-free tungsten−silylene complexes, $Cp'(CO)_2(H)W{=}SiH[C(SiMe_3)_3]$ ($Cp' = Cp^*$, C_5Me_4Et).[6] The silylene complexes contain a hydrido ligand that bears a significant interligand interaction with the silylene ligand.[7] Reactivity studies showed that the complexes react stoichiometrically with acetone[6] and nitriles[8] to produce hydrosilylation products (eqs 1 and 2). Interestingly, ^1H, ^{13}C, and ^{29}Si NMR spectroscopy studies reveal that **2** has a 3-center, 2-electron (3c-2e) W−H−Si bond, indicating that the W−H−Si structural moiety in **1** remains intact in the reaction. On the other hand, the acetonitrile hydrosilylation product **3** is a silyl complex containing a W−N−Si three-membered-ring structure, instead of the W−H−Si three-membered-ring structure found in **2**.

Tobita et al. proposed an interesting and new mechanism shown in Scheme 1 to account for the formation of **2** and **3**.[8,9] Initially, a substrate molecule coordinates to the Si center of the silylene ligand to form a base-stabilized silylene intermediate (**INT1**) in which the interligand interaction between the hydrido and silylene ligands is turned off. The hydrido ligand from the W center then migrates to the substrate carbon to give a tungsten−silyl intermediate **INT2**, which isomerizes to a more stable form (**2** and **3** for acetone and nitrile substrates, respectively). Since the intermediates **INT1** and **INT2** were not observed, the Tobita mechanism needs to be confirmed. It is also of interest to know why the reactions of **1** with acetonitrile and acetone give different hydrosilylation products and can catalytic hydrosilylations be achieved by using **1**. In this paper we report density functional theory calculations on the detailed reaction mechanisms of these reactions.

Computational Details

All calculations were performed using the Gaussian 03 package[10] with the density functional theory (DFT) method of B3LYP. Geometries were optimized with the following basis set: W, LanL2DZ with a set of f polarization functions;[11] Si, LanL2DZ with a set of d polarization functions;[12] and the rest of elements, 6-31G*. Frequency calculations were also performed on all the optimized structures with the same method to identify all the stationary points as minima (zero imaginary frequency) and transition states (one imaginary frequency) and to provide relative free energies (ΔG) at 298.15 K. Both the calculated relative free energies and electronic energies give the same conclusions. Therefore, in the text, we only report the calculated free energies, which include entropic contributions that are important for reactions involving more than one molecule although the contributions could be overestimated. The calculated relative electronic energies are given in the Supporting Information.

The B3LYP method together with the basis set described above was proved to be reliable in studies of many related

(2) (a) Waterman, R.; Hayes, P. G.; Tilley, T. D. *Acc. Chem. Res.* **2007**, *40*, 712. (b) Tilley, T. D. In *The Chemistry of Organosilicon Compounds*; Patai, S., Rappoport, Z., Eds.; Wiley & Sons: New York, 1989; pp 1415−1477. (c) Tilley, T. D. In *The Silicon-Heteroatom Bond*; Patai, S., Rappoport, Z., Eds.; Wiley & Sons: New York, 1991; p 245. (d) Sharma, H. K.; Pannell, K. H. *Chem. Rev.* **1995**, *95*, 1351. (e) Eisen, M. S. In *The Chemistry of Organosilicon Compounds*; Rappoport, Z., Apeloig, Y., Eds.; Wiley & Sons: New York, 1998; pp 2037−2128. (f) Okazaki, M.; Tobita, H.; Ogino, H. *J. Chem. Soc., Dalton Trans.* **2003**, 493. (g) Klei, S. R.; Tilley, T. D.; Bergman, R. G. *Organometallics* **2002**, *21*, 4648.

(3) Glaser, P. B.; Tilley, T. D. *J. Am. Chem. Soc.* **2003**, *125*, 13640.

(4) (a) Beddie, C.; Hall, M. B. *J. Am. Chem. Soc.* **2004**, *126*, 13564. (b) Hayes, P. G.; Beddie, C.; Hall, M. B.; Waterman, R.; Tilley, T. D. *J. Am. Chem. Soc*. **2006**, *128*, 428. (c) Beddie, C.; Hall, M. B. *J. Phys. Chem. A* **2006**, *110*, 1416. (d) Böhme, U. *J. Organomet. Chem.* **2006**, *691*, 4400.

(5) Chung, L. W. Ph.D. thesis, The Hong Kong University of Science and Technology (HK), 2006.

(6) Watanabe, T.; Hashimoto, H.; Tobita, H. *Angew. Chem., Int. Ed.* **2004**, *43*, 218.

(7) (a) Corey, J. Y.; Braddock-Wilking, J. *Chem. Rev.* **1999**, *99*, 175−292. (b) Nikonov, G. I. *J. Organomet. Chem.* **2001**, *635*, 24−36. (c) Lin, Z. *Chem. Soc. Rev.* **2002**, *31*, 239−245.

(8) Watanabe, T.; Hashimoto, H.; Tobita, H. *J. Am. Chem. Soc.* **2006**, *128*, 2176.

(9) Okazaki, M.; Jung, K. A; Satoh, K.; Okada, H.; Naito, J.; Akagi, T.; Tobita, H.; Ogino, H. *J. Am. Chem. Soc.* **2004**, *126*, 5060.

(10) Frisch, M. J.; Trucks, G. W.; Schlegel, H. B.; et al. *Gaussian 03*, Revision B.03; Gaussian, Inc.: Wallingford, CT, 2004. A complete author list is given in the Supporting Information.

(11) Ehlers, A. W.; Böhme, M.; Dapprich, S.; Gobbi, A.; Höllwarth, A.; Jonas, V.; Köhler, K. F.; Stegmann, R.; Veldkamp, A.; Frenking, G. *Chem. Phys. Lett.* **1993**, *208*, 111.

(12) Höllwarth, A.; Böhme, M.; Dapprich, S.; Ehlers, A. W.; Gobbi, A.; Jonas, V.; Köhler, K. F.; Stegmann, R.; Veldkamp, A.; Frenking, G. *Chem. Phys. Lett.* **1993**, *208*, 237.

CHART 1

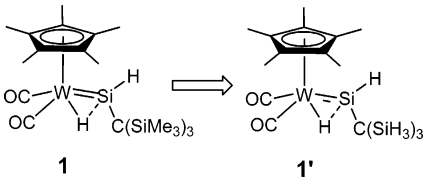

systems.[4,13−16] To further examine the effect of basis sets, a much larger basis set, SDDALL[17] with a set of f polarization functions for W[18] and 6-311+G** for all other atoms, was employed to perform the single-point calculations for several selected important structures. The relative energies, with respect to **5A**, of $\mathbf{TS_{A5-6}}$, **6A**, $\mathbf{TS_{A8-9}}$, **10A**, $\mathbf{TS_{A10-9}}$, and **3A** with the smaller basis set are 6.2, −17.8, 10.9, −1.4, 14.6, and −24.0 kcal/mol, respectively, and with the lager basis set are 6.3, −17.6, 10.5, −3.2, 14.5, and −25.7 kcal/mol. Similarly, the relative energies, with respect to **5B**, of $\mathbf{TS_{B5-6}}$, **6B**, $\mathbf{TS_{B8-9}}$, **10B**, $\mathbf{TS_{B10-9}}$, and **2B** with the smaller basis set are 9.5, −14.7, 7.6, −7.3, 1.9 and −32.2 kcal/mol, respectively, and with the lager basis set are 9.1, −16.6, 6.3, −8.4, 2.0, and −37.8 kcal/mol. The results show that the conclusions made are not affected by the use of different basis sets. The natural bond orbital (NBO) program,[19] which is implemented in Gaussian 03, was utilized to obtain NBO charges and Wiberg bond indices.[20] Since the methyl groups on the TMS are at positions remote from the reaction center, complex **1′** was employed as a model of **1** (Chart 1) in all the calculations.

Results and Discussion

Thermodynamic Stability of the Hydrosilylation Products. Before we discuss the mechanistic aspects of the two reactions mentioned in the Introduction, let us first see how the B3LYP theoretical method reproduces the X-ray crystal structure of Cp′-$(CO)_2$(H)W═SiH[$C(SiMe_3)_3$] (Cp′ = C_5Me_4Et).[6] The model complex **1′** calculated with this method is shown in Figure 1. The calculated structural parameters agree with the experimentally measured parameters very well, suggesting that the theoretical method used is acceptable. The calculated Si−H_b distance (1.676 Å) of **1′** is shorter than the silicon−hydrogen separation (1.802 Å) found in (η^5-C_5H_4Me)$(CO)_2$(H)Mn-$(SiFPh_2)$,[21] suggesting that there is a significant Si−H interaction in the complex.[7] Here, H_b stands for the bridging hydrido ligand. Although the Si−H_b distance in the complex is longer than the average bond length (1.48 Å) in hydrosilanes,[7a] it is almost the same as that found in Cp*(dmpe)Mo(H)$(SiEt_2)$ (1.68 Å),[22] featuring a typical M−H−Si 3c-2e bonding interaction.

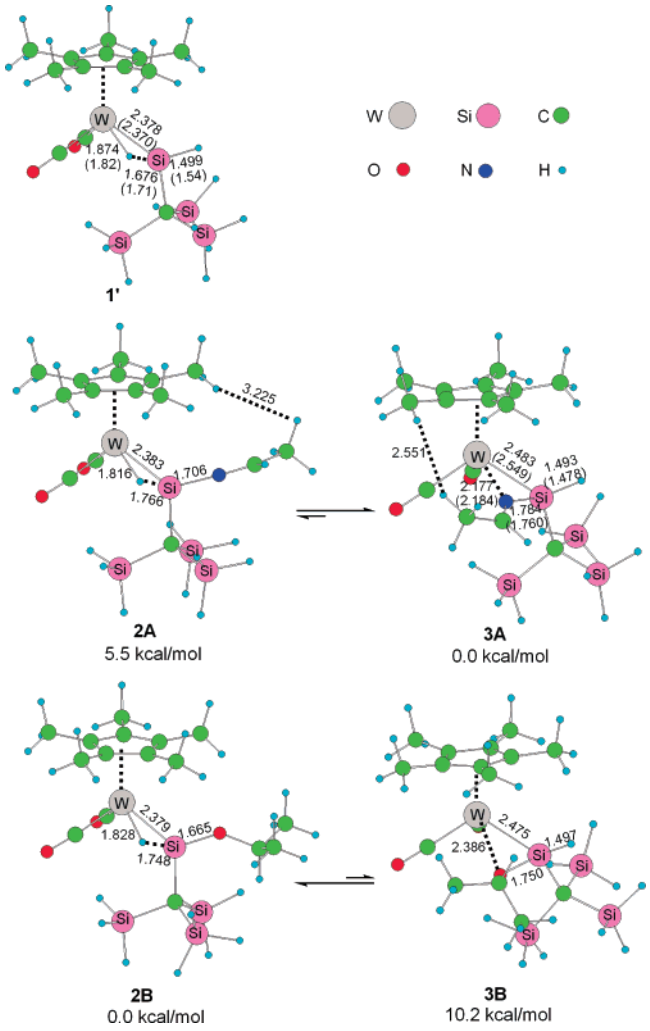

FIGURE 1. Selected bond distances (in Å) and relative free energies calculated for **1′**, **2A**, **3A**, **2B**, and **3B** together with the experimentally observed bond distances (in parentheses) in Cp′$(CO)_2$(H)W═SiH-[$C(SiMe_3)_3$] and Cp′$(CO)_2$W−Si(N═CHMe)H[$C(SiMe_3)_3$] (Cp′ = C_5Me_4Et).

Figure 1 also shows the calculated structures of the two isomeric products **2** and **3**. **A** and **B** represent the acetonitrile and acetone hydrosilylation products, respectively. The calculations indicate that the nitrogen-bridged isomer **3A** is about 5.5 kcal/mol more stable than the hydrido-bridged isomer **2A** for the reaction of nitrile, and the hydrido-bridged isomer **2B** is about 10.2 kcal/mol more stable than the oxygen-bridged isomer **3B** for the reaction of acetone. These results are in excellent agreement with observations by Tobita et al. It should be noted that pivalonitrile also reacted with **1**, but gave a mixture of **2A**-like and **3A**-like. The **3A**-like complex finally isomerizes to

(13) (a) Chung, L. W.; Wu, Y.-D.; Trost, B. M.; Ball, Z. T. *J. Am. Chem. Soc.* **2003**, *125*, 11578. (b) Chung, L. W.; Lee, H. G.; Li, Z.; Wu, Y.-D. *J. Org. Chem.* **2006**, *71*, 6000. (c) Wu, Y.-D.; Chung, L. W.; Zhang, X.-H. In *Computational Modeling for Homogeneous and Enzymatic Catalysis*; Morokuma, K., Musaev, J., Eds.; Wiley-VCH: Weinheim, Germany, 2007, pp 285−316.

(14) (a) Ray, M.; Nakao, Y.; Sato, H.; Sakaba, H.; Sakaki, S. *J. Am. Chem. Soc.* **2006**, *128*, 11927. (b) Sakaki, S.; Takayama, T.; Sumimoto, M.; Sugimoto, M. *J. Am. Chem. Soc.* **2004**, *126*, 3332.

(15) (a) Tuttle, T.; Wang, D.; Thiel, W.; Köhler, J.; Hofmann, M.; Weis, J. *Organometallics* **2006**, *25*, 4504. (b) Bandini, M.; Bernardi, F.; Bottoni, A.; Cozzi, P. G.; Miscione, G. P.; Umani-Ronchi, A. *Eur. J. Org. Chem.* **2003**, 2972. (c) Xue, P.; Zhu, J.; Liu, S. H.; Huang, X.; Ng, W. S.; Sung, H. H. Y.; Williams, I. D.; Lin, Z. Y.; Jia, G. C. *Organometallics* **2006**, *25*, 2344.

(16) (a) Besora, M.; Maseras, F.; Lledós, A.; Eisenstein, O. *Inorg. Chem.* **2002**, *41*, 7105. (b) Besora, M.; Maseras, F.; Lledós, A.; Eisenstein, O. *Organometallics* **2006**, *25*, 4748.

(17) (a) Bergner, A.; Dolg, M.; Kuechle, W.; Stoll, H.; Preuss, H. *Mol. Phys.* **1993**, *80*, 1431. (b) Dolg, M.; Wedig, U.; Stoll, H.; Preuss, H. *J. Chem. Phys.* **1987**, *86*, 866.

(18) (a) Martin, J. M. L.; Sundermann, A. *J. Chem. Phys.* **2001**, *114*, 3408. (b) Iron, M. A.; Lucassen, A. C. B.; Cohen, H.; van der Boom, M. E.; Martin, J. M. L. *J. Am. Chem. Soc.* **2004**, *126*, 11699.

(19) Glendening, E. D.; Reed, A. E.; Carpenter, J. E.; Weinhold, F. *NBO* Version 3.1.

(20) Wiberg, K. B. *Tetrahedron* **1968**, *24*, 1083.

(21) Schubert, U.; Ackermann, K.; Wörle, B. *J. Am. Chem. Soc.* **1982**, *104*, 7378.

(22) Mork, B. V.; Tilley, T. D.; Schultz, A. J.; Cowan, J. A. *J. Am. Chem. Soc.* **2004**, *126*, 10428.

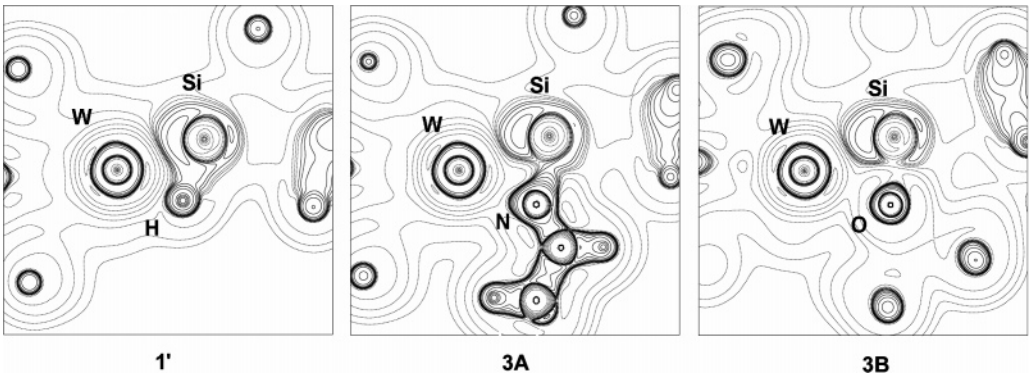

FIGURE 2. Plots of the Laplacian of electron densities for **1′**, **3A**, and **3B** on the W−X−Si (X = H, N, O) planes.

the **2A**-like complex. From the calculated structures of **2A** and **3A**, we expect that the larger steric hindrance of the *tert*-butyl substituent in the pivalonitrile substrate may switch the isomeric preference.[8]

To understand the bonding interactions in the W−H−Si, W−N−Si, and W−O−Si three-membered-ring structures, we obtained the Laplacian plots of electron density for **1′**, **3A**, and **3B** (Figure 2). In the Laplacian plot of electron density for **1′**, significant concentration of electron density between the silicon atom and the bridging hydrogen atom can be found, revealing that strong Si−H interaction exists in addition to the metal−hydrido bonding interaction. The bridging hydrido ligand simultaneously interacts with the metal center and the silylene silicon, suggesting that there is a three-center, two-electron (3c-2e) W−H−Si bond. The Laplacian plots of **2A** and **2B**, not shown in the figure, depict similar bonding feature as that of **1′**, suggesting that both **2A** and **2B** also have a 3c-2e W−H−Si bond. The reasons for the silylene ligands in **1′**, **2A**, and **2B** being able to interact with the hydrido ligand of the Cp*W-$(CO)_2$(H) fragment are as follows. In metal−silylene complexes, there is an important resonance contributor that establishes a positive charge at silicon, rendering the silicon center capable of interacting with the hydrido ligand.[4b] With the hydrido-bridged complexes, introducing an additional ligand to the silicon center can easily break the silylene−hydrido interaction. For example, no silylene−hydrido interaction can be found in the Cp*$(CO)_2$(H)W═SiR_2·py in which a pyridine coordinates to the silylene ligand.[23] Similarly, introducing an additional ligand to the metal center breaks the W−H interaction and forces the hydrido ligand to completely migrate to the silylene silicon center to form a silyl ligand. For example, no 3c-2e W−H−Si bond can be found in Cp*$(CO)_3WSiH_2[C(SiMe_3)_3]$ in which one more CO ligand is introduced to the W center.[6]

For **3A** and **3B**, each of the bridging ligands shows a strong bonding interaction with the silicon center and forms a dative bond to the metal center (Figures 1 and 2). Despite the similarity of **3A** and **3B** in bonding, they have very different stabilities. **3A** is more stable than its hydrido-bridged isomer **2A**. However, **3B** is less stable than its hydrido-bridged isomer **2B**. We believe that in **3A** or **3B** the dative bond of the bridging ligand to the metal center plays an important role in determining the relative stabilities. In **3A**, the N→W dative bond is short and strong. There is significant concentration of electron density around the bridging N toward the W metal center (Figure 2). In **3B**, the W−O distance is long, indicating a weak O→W dative bond.

(23) Sakaba, H.; Tsukamoto, M.; Hirat, T.; Kabuto, C.; Horino, H. *J. Am. Chem. Soc.* **2000**, *122*, 11511.

SCHEME 2. Schematic Illustration of the Bonding Interaction between the Bridging Group and the W Center in 3A and 3B

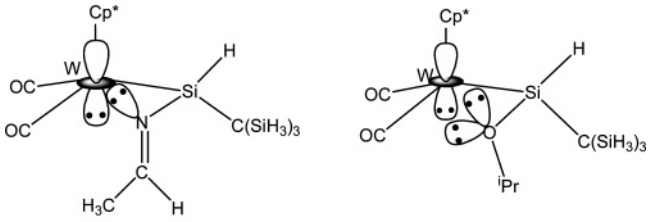

Unlike in **3A**, there is no significant concentration of electron density around the bridging O toward the W metal center in **3B** (Figure 2). The calculated Wiberg bond indices of W−N in **3A** and W−O in **3B** are 0.501 and 0.288, respectively, consistent with the arguments given above. Scheme 2 attempts to illustrate the difference in the metal−bridging ligand bonding interactions between **3A** and **3B**. The formally d^4 W(II) center of **3B** possesses a filled nonbonding d_{z^2} orbital, which creates repulsive interaction with the extra lone pair of the bridging oxygen atom. The repulsive interaction significantly weakens the O→W dative bond and therefore destabilizes the alkoxide-bridged structural form, making **3B** less stable than its hydrido-bridged isomer **2B**. We also examined the steric effect on the relative stability of **3B** with respect to **2B** caused by the bulky −O^{i}Pr group. A smaller alkoxide group, −OMe, was tested. The calculated energy difference between $\mathbf{2B_{Me}}$ and $\mathbf{3B_{Me}}$ is reduced to 7.0 kcal/mol. Despite the reduction in the energy difference, the hydrido-bridged structure is still more favorable. Therefore, we can conclude that it is the electronic factor that accounts for the stability difference.

Mechanistic Aspects of the Hydrosilylation Reactions. Scheme 3 shows four possible reaction modes for the reactions of **1′** with the substrates acetonitrile and acetone. The first one is the mechanism proposed by Tobita (see also Scheme 1). Coordination of a substrate molecule to the silylene silicon center breaks the silylene−hydrido interaction followed by migration of the hydrido ligand to the silylene-activated substrate through a 5-membered-ring transition state to give a tungsten−silyl intermediate. The second one considers [2+3] interaction between a substrate molecule and a 16-electron metal−silyl fragment formed by breaking the W−H interaction in the W−H−Si bridging moiety of **1′**. This mechanism is named the Silyl Hydride Migration to differentiate it from the Metal Hydride Migration that was proposed by the Tobita group. The third one (Silyl Migration) also starts with a 16-electron metal−

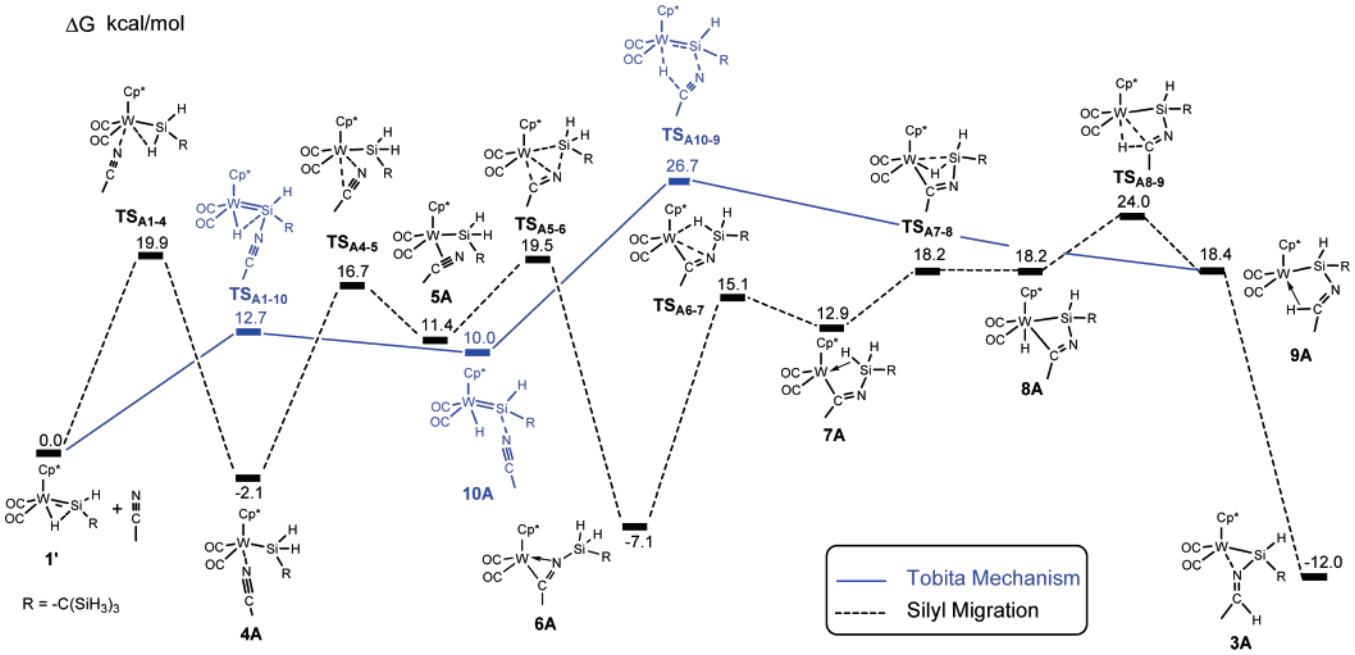

FIGURE 3. Calculated free energy profiles of the Tobita mechanism and the Silyl Migration mechanism for the reaction of acetonitrile with **1′**. The relative free energies are given in kcal/mol.

SCHEME 3. Four Possible Reaction Modes of Hydrosilylation of Unsaturated Compounds (EX) with the Tungsten Complex 1′ [a]

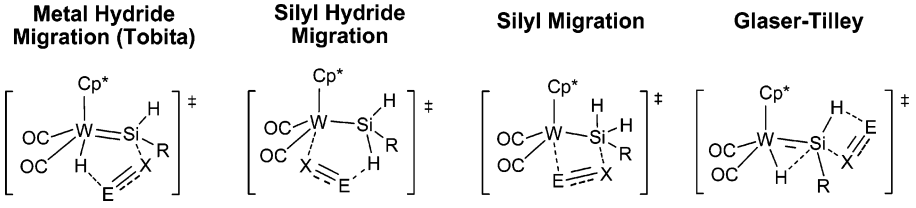

[a] E = CMe_2 when X = O and *E* = CMe when X = N.

silyl fragment and involves a silyl group migration similar to that in the modified Chalk−Harrod mechanism proposed for many metal-mediated hydrosilylation reactions.[1] The forth one, the Glaser−Tilley mechanism, is the [2_σ+2_π] addition of an Si−H bond of the silylene moiety across the multiple bond of a substrate molecule.[3]

(a) The Tobita and Silyl Migration Mechanisms. Our calculations of the four reaction mechanisms discussed above show that the Silyl Hydride Migration mechanism and the Glaser−Tilley mechanism, which will be discussed in the next section, are less favorable than the Tobita and Silyl Migration mechanisms. Therefore, the Tobita mechanism and the Silyl Migration mechanism will be discussed in more detail first.

On the basis of the Tobita and Silyl Migration mechanisms, we calculated the detailed reaction pathways for the reactions of **1′** with acetonitrile and acetone. The calculated free energy profiles for the detailed reaction pathways are given in Figures 3 and 4, respectively. Selected calculated geometries are shown in Figure 5. The total energy of **1′** and the substrate, acetonitrile or acetone, is set to zero as the reference point.

Figure 3 shows the calculated free energy profiles on the basis of the Tobita and Silyl Migration mechanisms for the reaction of **1′** with acetonitrile. In the Tobita mechanism, coordination of acetonitrile to the electrophilic Si center of the silylene ligand in **1′** through **TS$_{A1-10}$** affords the base-stabilized silylene intermediate **10A**. The next step is the hydride migration from the metal center to the carbon center of acetonitrile to form **9A** via **TS$_{A10-9}$**. The rate-determining step of the Tobita mechanism is the acetonitrile coordination to the silylene Si center followed by the hydride migration. The activation free energy calculated for the Tobita mechanism is about 26.7 kcal/mol. In **9A**, the newly formed C−H bond has an agostic interaction with the W center. Finally, **9A** undergoes a structural rearrangement to give the more stable isomer **3A**, the observed product, with a negligible barrier.

The Silyl Migration mechanism is more complicated and involves more steps (Figure 3). The coordination of acetonitrile to the W center required a higher barrier (19.9 kcal/mol) than that to the Si center. However, the formation of the silyl intermediate **4A** is exergonic. This result is consistent with the experimental observation that the silyl complex Cp*$(CO)_3WSiH_2$-$[C(SiMe_3)_3]$ was formed when CO was added to the solution of **1**.[6] The **4A** → **5A** step is a process related to the conversion of the acetonitrile ligand from an end-on coordination mode to a side-on coordination mode. From the side-on intermediate **5A**, a silyl migration occurs to give **6A** via transition state **TS$_{A5-6}$**. In this silyl migration step, a new W−C bond is formed. Although it is relatively stable, **6A** is not the observed product in the experiment reported in 2006.[8] In 2007, Tobita and co-workers reported the synthesis and characterization of N-silylated η^2-iminoacyl tungsten complexes, which have a three-membered metallacycle structure like **6A**. The characterization

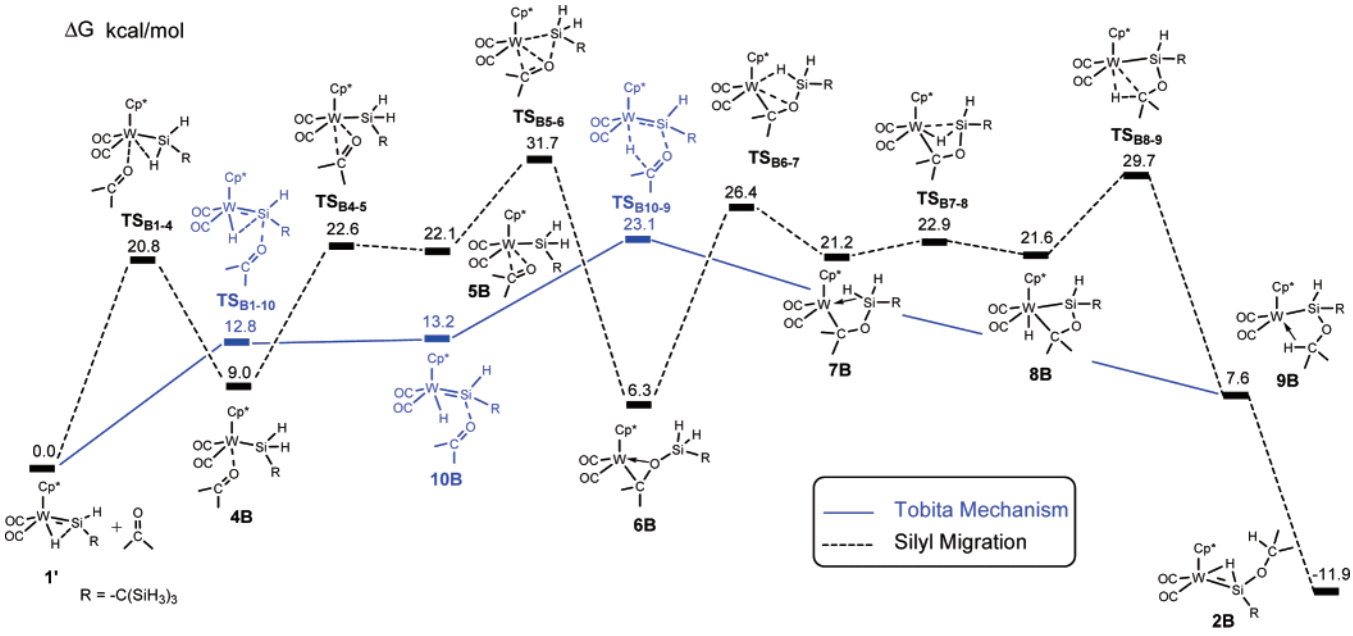

FIGURE 4. Calculated free energy profiles of the Tobita mechanism and the Silyl Migration mechanism for the reaction of acetone with **1′**. The relative free energies are given in kcal/mol.

of these compounds is in agreement with our calculation result that **6A** is a stable intermediate and supports the proposed Silyl Migration mechanism.[24] It undergoes a series of tungsten-mediated steps (formation of the agostic species **7A** having W−η^2-H−Si interaction, oxidative addition of the η^2-H−Si to the W metal center followed by a reductive elimination) to transfer a hydrogen atom from Si to C, yielding the observed product **3A**. The rate-determining barrier for the acetonitrile hydrosilylation in the Silyl Migration mechanism is about 31.1 kcal/mol (**6A** → **TS$_{A8-9}$**).

The highest free energy transition state in the Silyl Migration mechanism, **TS$_{A8-9}$**, has a relative free energy of 24.0 kcal/mol. **TS$_{A8-9}$** is lower in energy than **TS$_{A10-9}$**, the highest free energy transition state in the Tobita mechanism, suggesting that the Silyl Migration mechanism is more favorable. The reason for this conclusion is as follows. **6A** is a species easily formed in the reaction mixture because the overall barrier for its formation is less than 20 kcal/mol. Therefore, the energetic span[25] for the Tobita mechanism corresponds to the energy difference between **TS$_{A10-9}$** and **6A**, and is about 33.8 kcal/mol. The energetic span for the Silyl Migration mechanism corresponds to the energy difference between **TS$_{A8-9}$** and **6A**, and is about 31.1 kcal/mol, which is smaller than that for the Tobita mechanism.

Figure 4 shows the calculated free energy profiles on the basis of the Tobita and Silyl Migration mechanisms for the reaction of **1′** with acetone. The Tobita mechanism is clearly more favorable than the Silyl Migration mechanism. The overall reaction barrier calculated for the Tobita mechanism is 23.1 kcal/mol while it is 31.7 kcal/mol for the Silyl Migration mechanism. The overall reaction barrier of the Tobita mechanism for the reaction of acetone is noticeably lower than that for the reaction of acetonitrile (**TS$_{B10-9}$** versus **TS$_{A10-9}$**), reflecting the higher reactivity of carbonyl over nitrile toward hydride ligand. The results are consistent with the experimental observation that the acetone hydrosilylation is faster than the acetonitrile hydrosilylation.[6,8]

Why do acetonitrile and acetone hydrosilylations proceed via different mechanisms? In the Tobita mechanism, the substrate, acetone or acetonitrile, coordinates to the Si center of **1** (or **1′**). The substituents on the substrate are far away from the metal center. Therefore, the steric repulsion between the substituents and the metal-bonded ligands (Cp* and CO) does not differ much for the two substrates. In the substrate-coordinated intermediates **10A** and **10B**, the Si−N (1.995 Å) and Si−O (2.006 Å) distances are similar (Figure 5). In the hydride migration transition structures **TS$_{A10-9}$** and **TS$_{B10-9}$**, the steric crowdedness is also similar (Figure 5). Electronically, acetone has lower LUMO (−0.011 au) than acetonitrile (0.037 au). The carbon center of carbonyl (+0.42) carries more positive charge than that of nitrile (+0.21). Therefore, the carbon center of the carbonyl group in acetone is much more electrophilic than the carbon center in acetonitrile. As a result, hydrosilylation of acetone with **1** (or **1′**) has a lower barrier (23.1 kcal/mol) than that of acetonitrile (26.7 kcal/mol) in the Tobita mechanism.

In the Silyl Migration mechanism, the steric effect, however, plays an important role because direct coordination of the substrate, acetone or acetonitrile, to the metal center initiates the reaction. In the precursor π complexes **5A** and **5B** (Figures 3, 4, and 5) that lead to the silyl migration, the W−C distance in **5B** (2.452 Å) is much longer than that in **5A** (2.226 Å). In the reaction of acetone, **5B** experiences a significant steric repulsion between one methyl group of the acetone and the Cp* ligand. In addition, the other methyl group of acetone, which points away from the metal center, has repulsive interactions with the −C(SiH$_3$)$_3$ group on the silylene ligand (Figure 5). The results of calculation show that the π precursor complex **5B** is high in energy, 22.1 kcal/mol with respect to the reference point, **1′** and acetone. The silyl migration transition state **TS$_{B5-6}$** lies even higher in energy, 31.7 kcal/mol with respect to the reference point (Figure 4). In contrast, the π precursor complex

(24) Suzuki, E.; Komuro, T.; Okazaki, M.; Tobita, H. *Organometallics* **2007**, *26*, 4379.

(25) (a) Amatore, C.; Jutand, A. *J. Organomet. Chem.* **1999**, *576*, 254. (b) Kozuch, S.; Amatore, C.; Jutand, A.; Shaik, S. *Organometallics* **2005**, *24*, 2319.

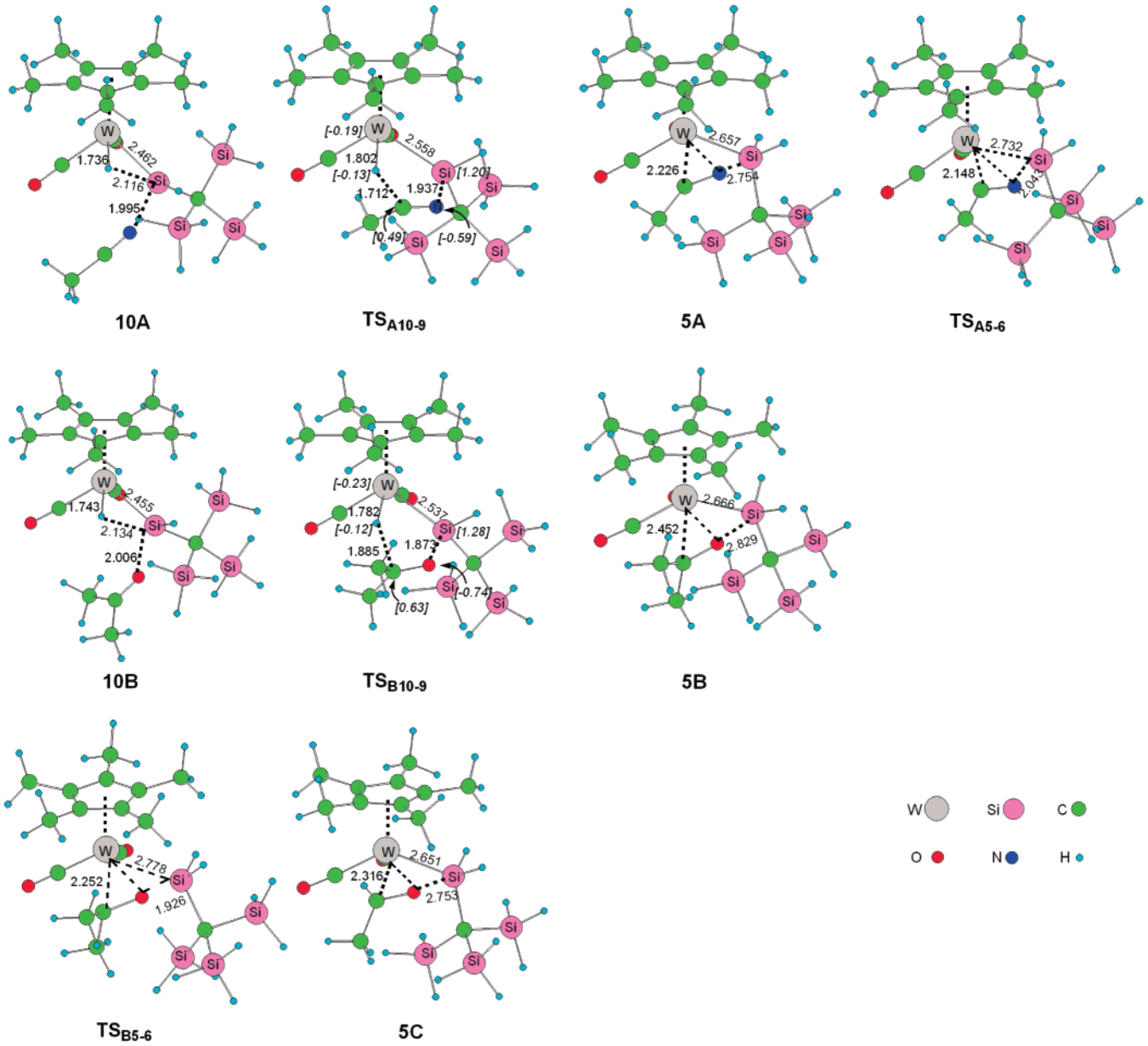

FIGURE 5. Optimized structures of selected species involved in the Tobita mechanism and the Silyl Migration mechanism. Distances are in Å; NBO charges are shown in brackets.

5A in the reaction of acetonitrile experiences much less steric repulsion because acetonitrile can use one of its π bonds for metal coordination and has the methyl substituent pointing away from the Cp* ligand and the $-C(SiH_3)_3$ substituent on the silylene ligand. To support the steric argument here, we did calculations using acetaldehyde as the substrate and found that the W−C distance is shortened to 2.316 Å in the precursor π complex **5C** (Figure 5). The relative free energy of the corresponding silyl migration transition state **TS$_{C5-6}$** decreases to 22.2 kcal/mol with respect to the reference point. Clearly, the silyl migration mechanism of the acetone reaction is significantly disfavored by steric interactions.

(b) The Silyl Hydride Migration and Glaser−Tilley Mechanisms. Figure 6 shows the rate-determining transition states calculated for the Silyl Hydride Migration mechanism and the Glaser−Tilley mechanism. The rate-determining transition states **TS$_{A4-9}$** (acetonitrile) and **TS$_{B4-9}$** (acetone) in the Silyl Hydride Migration mechanism (Figure 6) are respectively higher in free energies than the rate-determining transition states **TS$_{A10-9}$** (acetonitrile) and **TS$_{B10-9}$** (acetone) in the Tobita mechanism (Figures 3 and 4). We believe that these results are related to the poorer basicity of the hydride acting to nucleophilically attack the acetonitrile or acetone carbon center in the Silyl Hydride Migration transition state (**TS$_{A4-9}$** or **TS$_{B4-9}$**). NBO population analysis indeed shows that the attacking hydrides in **TS$_{A4-9}$** and **TS$_{B4-9}$** carry less negative charge than those in **TS$_{A10-9}$** and **TS$_{B10-9}$** (Figures 5 and 6).

In the Glaser−Tilley $[2_\sigma+2_\pi]$ mechanism, the rate-determining transition states **TS$_{A11-2}$** (acetonitrile) and **TS$_{B11-2}$** (acetone) were found to be 35.7 and 33.3 kcal/mol, respectively, higher in free energy than their reference points. These results clearly suggest that the Glaser−Tilley $[2_\sigma+2_\pi]$ mechanism is unfavorable here. It was mentioned in the Introduction that a cationic ruthenium−silylene complex catalyzes hydrosilylation of alkenes via the Glaser−Tilley $[2_\sigma+2_\pi]$ mechanism. A recent experimental and theoretical study of osmium−silylene-medi-

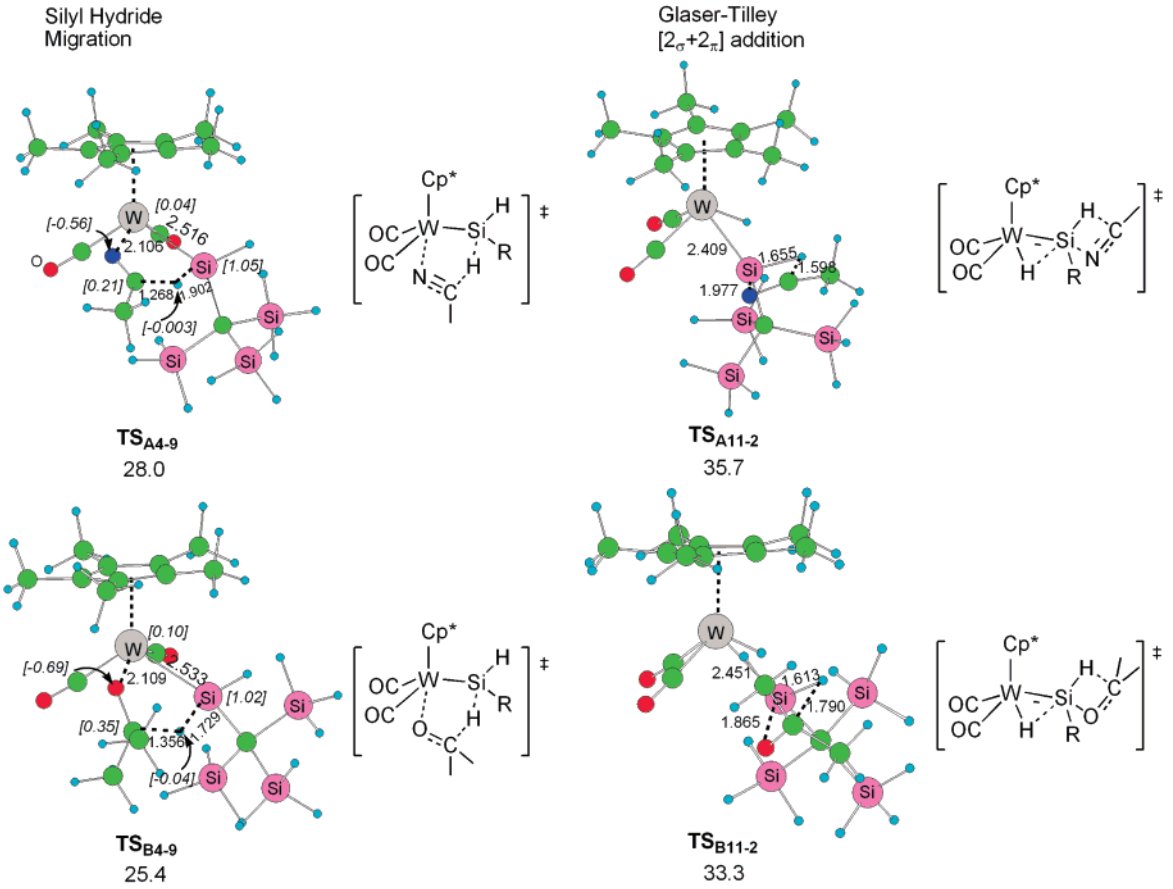

FIGURE 6. The rate-determining transition state structures calculated for the Silyl Hydride Migration mechanism and the Glaser−Tilley mechanism. Distances are in Å; NBO charges are shown in brackets; relative free energies are in kcal/mol.

ated ethylene hydrosilylation showed that large positive charge on Si of the silylene ligand promoted the Glaser−Tilley mechanism.[4b] The study found that cationic silylene complexes contained a more positive Si center and reacted with olefin via the Glaser−Tilley mechanism, while neutral silylene complexes contained a much less positive Si center and reacted with olefin via other mechanisms. The higher barriers in the Glaser−Tilley $[2_\sigma+2_\pi]$ mechanism are also likely related to the fact that the tungsten silylene complexes studied here are neutral.

Can the Reactions Be Made Catalytic? **1** reacts with the inactive acetonitrile to yield hydrosilylation product **3** and with acetone to give **2** (eqs 1 and 2). Both the hydrosilylation reactions are stoichiometric. Here, we are interested in the question of whether the reactions can be made catalytic. If **3** and **2** each could further react with a silane molecule to regenerate **1** and release the acetonitrile- and acetone-hydrosilylated species, the catalytic reactions would become possible.

Taking acetonitrile as an example, we considered four possible pathways for the regeneration of **1′** from the reaction of **3A** with SiH_4, as shown in Scheme 4. For simplicity and convenience, we used the simplest hydrosilane SiH_4, instead of $H-SiH_2[C(SiH_3)_3]$, in the model calculations. The first pathway considers oxidative addition of SiH_4 to the W complex **3A** and subsequent reductive elimination to release the acetonitrile-hydrosilylated species. The second pathway considers a direct σ-bond metathesis between **3A** and SiH_4 (Scheme 4). An alternative pathway is that **3A** isomerizes to a 16-electron species by dissociation of the nitrogen atom and then undergoes σ-bond metathesis with SiH_4. Attempts to locate such a transition state led to $\mathbf{TS_{A3-1}}$. The third and forth pathways first consider isomerization of **3A** and then σ-bond metathesis (Scheme 4). It is well-known that σ-bond metathesis typically takes place in d^0 early transition metal complexes[26,27] while oxidative addition often occurs on electron-rich late transition metal centers.[28]

Table 1 lists the calculated relative free energies calculated for the transition states shown in Scheme 4 for both the substrates acetonitrile and acetone. Figure 7 gives the optimized transition state structures. The results show that all the transition states calculated are high in energy, suggesting that catalytic processes using the tungsten complexes **1** and **1′** as the catalysts for hydrosilylation of acetonitrile or acetone are unlikely to be possible. We failed to locate the transition states in the oxidative addition pathway, likely due to that the tungsten center in **1** has already a very crowded ligand environment. Interestingly, $\mathbf{TS_{A6-1}}$ is not lying very high in energy (Table 1). Considering that we used the simplest silane model, SiH_4, in the calculations, we believe that when a more realistic silane is used, the relevant transition state would be even less stable due to the steric effect.

We also studied the effect of the metal center and ligands on the kinetic barriers of the regeneration processes. We took $\mathbf{TS_{A6-1}}$ (Scheme 4) as our starting point to study the effect because $\mathbf{TS_{A6-1}}$ is the most accessible transition state among

(26) Lin, Z. *Coord. Chem. Rev.* **2007**, *251*, 2280.
(27) (a) Sadow, A. D.; Tilley, T. D. *Angew. Chem., Int. Ed.* **2003**, *42*, 803. (b) Sadow, A. D.; Tilley, T. D. *Organometallics* **2003**, *22*, 3577.
(28) (a) Chan, D.; Duckett, S. B.; Heath, S. L.; Khazal, I. G.; Perutz, R. N.; Sabo-Etienne, S.; Timmins, P. L. *Organometallics* **2004**, *23*, 5744. (b) Karshtedt, D.; Bell, A. T.; Tilley, T. D. *Organometallics* **2006**, *25*, 4471.

SCHEME 4. Four Possible Pathways for Regeneration of 1′ (here 1H Due to the Use of SiH_4 as the Model Hydrosilane) and Release of the Acetonitrile-Hydrosilylated Species

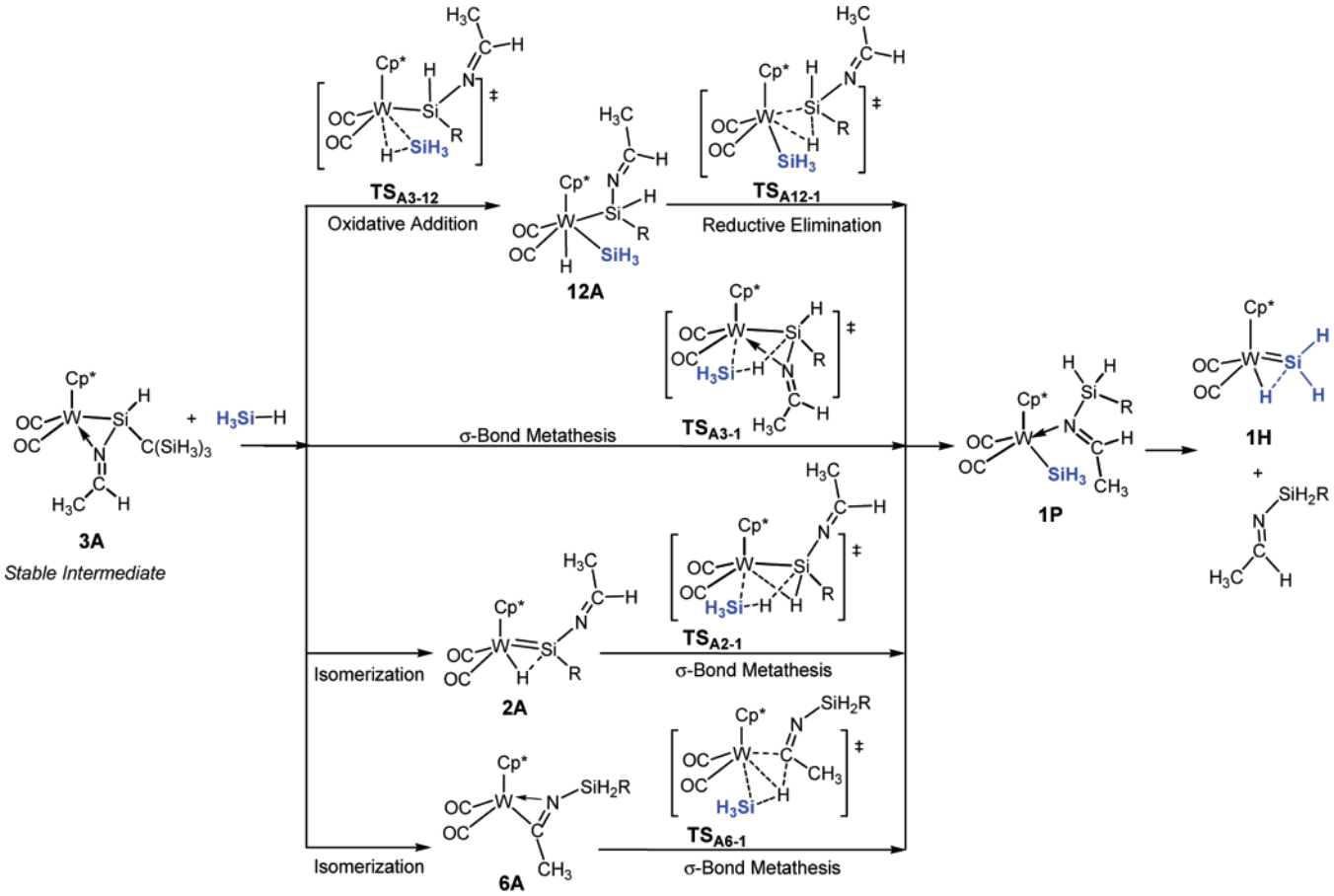

SCHEME 5. Summary of the Stoichiometric Hydrosilylation of Acetonitrile and Acetone with the Tungsten Silylene Complex 1

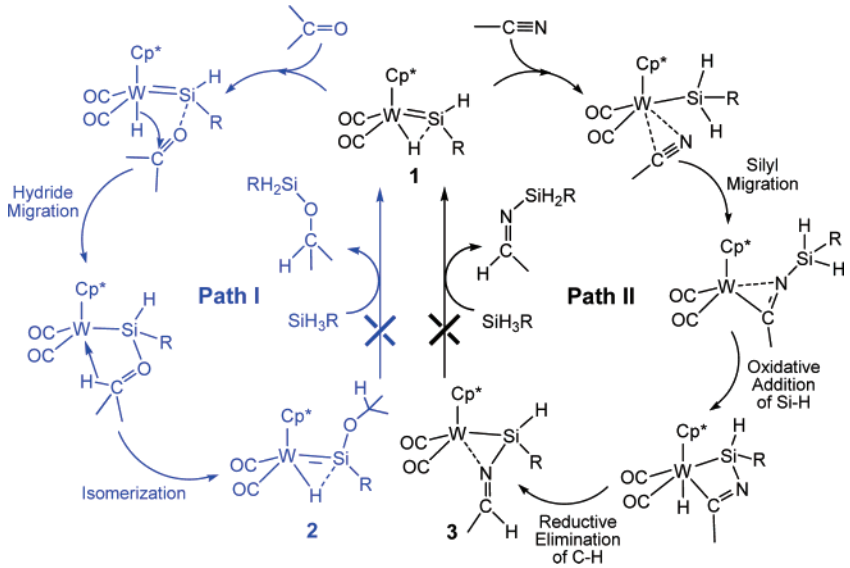

those studied (Table 1). First, we replaced Cp* in **TS$_{A6-1}$** with the less bulky Cp ligand and optimized the corresponding transition state. We found that the relative free energy of this Cp-based transition state is 27.6 kcal/mol with respect to its reference point, almost no change when compared with that (27.4 kcal/mol, Table 1) of **TS$_{A6-1}$**. Then, we replaced the WCp* moiety with MoCp and found that the relative free energy of this MoCp-based transition state was 27.1 kcal/mol, again not much change when compared with that of **TS$_{A6-1}$**. We also replaced the $(CO)_2$WCp* fragment with (dmpe)WCp and (dmpe)MoCp.[22,29] The relative free energies of these (dmpe)-WCp- and (dmpe)MoCp-based transition states are 30.5 and 31.4 kcal/mol, respectively, greater than that of **TS$_{A6-1}$**. All these additional calculations lead us to conclude that a catalytic

(29) Mork, B. V.; Tilley, T. D. *J. Am. Chem. Soc.* **2001**, *123*, 9702.

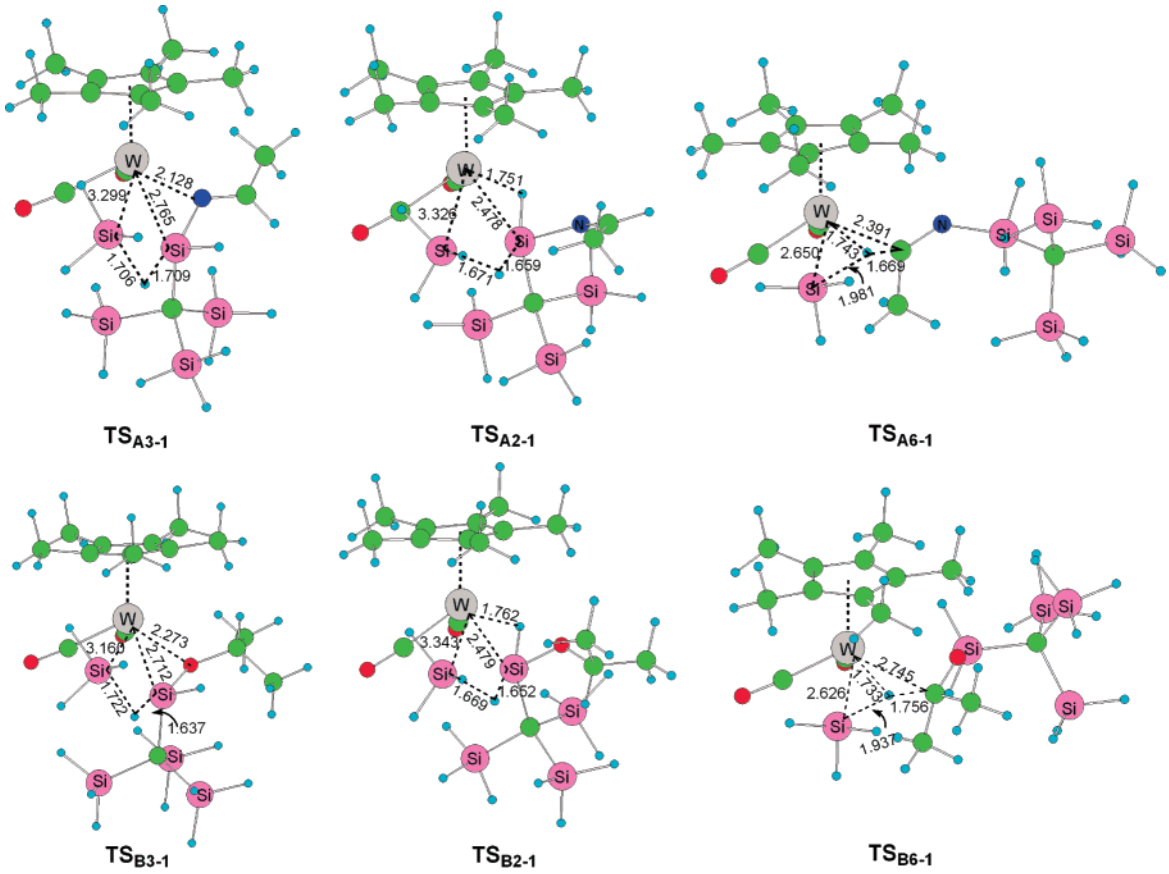

FIGURE 7. Optimized transition structures shown in Scheme 4. Distances are given in Å.

TABLE 1. The Relative Free Energies (kcal/mol) Calculated for the Transition States Shown in Scheme 4[a]

acetonitrile	**3A** + SiH_4	TS_{A3-12}	TS_{A3-1}	TS_{A2-1}	TS_{A6-1}
	−12.0	cannot be located	59.0	46.1	27.4
acetone	**2B** + SiH_4	TS_{B3-12}	TS_{B3-1}	TS_{B2-1}	TS_{B6-1}
	−11.9	cannot be located	67.2	37.8	36.8

[a] The total energy of **1′**, SiH_4, and the substrate, acetonitrile or acetone, is set to zero as the reference point.

hydrosilylation process with the neutral group VI metal−silylene complexes is difficult to achieve.

Conclusions

Theoretical calculations on the mechanisms of the stoichiometric hydrosilylation of acetone and acetonitrile with a neutral hydrido(hydrosilylene)tungsten complex (**1**) have been carried out. Scheme 5 summarizes the findings of this work. For the reaction of acetone, the Tobita mechanism (Path I), also called the Hydride Migration mechanism, is the most favorable. An acetone molecule is first coordinated to the silicon center of the silylene ligand in **1**, leading to the breaking of the silylene−hydrido interaction. Then, the hydrido ligand nucleophilically attacks the carbon center of the acetone molecule to complete the hydride migration to give an intermediate. The intermediate finally isomerizes to the hydrosilylation product (**2**). For the reaction of acetonitrile, the Silyl Migration mechanism (Path II) was found to be the most favorable. An acetonitrile is first coordinated to the metal center, leading to the breaking of the metal−hydrido bond to form a silyl ligand. From an η^2-acetonitrile coordinated intermediate, silyl migration occurs followed by oxidative addition of an Si−H bond on the metal center and then reductive elimination to give the hydrosilylation product (**3**).

The calculation results show that both electronic and steric factors favor the Tobita (Hydride Migration) mechanism for the reaction of acetone. Electronically, the carbon center of acetone is electrophilic enough to facilitate the rate-determining hydride migration step. Sterically, the Tobita mechanism allows a minimal repulsive interaction between the substituents on the acetone and the ligands around the metal centers. For the reaction of acetonitrile, the steric factor becomes less crucial. Electronically, the carbon center of the nitrile is not electrophilic enough. Therefore, the Silyl Migration mechanism, instead of the Tobita mechanism, is operative.

We also explored the feasibility of making the hydrosilylation reactions of the neutral tungsten complex catalytic. We found that the barriers to convert the hydrosilylation products **2** and **3** back to **1** by reacting with hydrosilanes are very high. Thus, the chance for this neutral tungsten−silylene complex to catalyze a hydrosilylation of unsaturated compounds is very small.

Acknowledgment. We thank the Research Grants Council of Hong Kong (N-HKUST 623/04 and HKUST 602304) for financial support.

Supporting Information Available: Complete ref 10, as well as Cartesian coordinates and electronic energies of all the calculated structures. This material is available free of charge via the Internet at http://pubs.acs.org.

JO701649M